

## Experimental Study of Self-Compacting Reinforced Concrete Hollow Beams Using Recycled Aggregate under Torsion



Ahmed Fadhil Kadhim Alfuraiji<sup>\*</sup>, Jamal Abdulsamad Khudhair<sup>\*</sup>

Civil Engineering Department, Basrah Health Directory, Basrah University, Basrah 61004, Iraq

Corresponding Author Email: [Ahmed.alnawrs7@gmail.com](mailto:Ahmed.alnawrs7@gmail.com)

Copyright: ©2024 The authors. This article is published by IETA and is licensed under the CC BY 4.0 license (<http://creativecommons.org/licenses/by/4.0/>).

<https://doi.org/10.18280/acsm.480403>

### ABSTRACT

**Received:** 2 May 2024

**Revised:** 28 July 2024

**Accepted:** 7 August 2024

**Available online:** 30 August 2024

#### Keywords:

*self-compacting concrete (SCC), beams, recycled aggregate concrete (RCA), torsion, crack, reinforcement, angles of twist, ultimate load*

This research work aims to investigate experimentally the torsional behaviour of self-compacting reinforced concrete hollow beams with recycled concrete aggregate. Twelve beams were cast and tested. The beams have the same dimensions, and the variables that were investigated include, recycled aggregate content, longitudinal reinforcement, and transverse reinforcement. The test results revealed that for all beams no significant difference in behaviour was identified when comparing beams with recycled aggregate with those with normal aggregate. All the beams exhibited almost similar linear torque-rotation behaviour, but beams with RCA showed lower cracking torque and the twist angle depended on the replacement ratio of RCA. Beams without any reinforcement failed suddenly and separated into two parts, while beams with longitudinal bars showed brittle torsional failure, beams with both longitudinal and transverse reinforcement showed an increasing post-cracking behaviour with the formation of an increase in the number of helical and diagonal cracks.

## 1. INTRODUCTION

SCC is a type of concrete that exhibits increased deformability and resistance to segregation. Initially, it was created in Japan in 1986 [1]. The substance has the ability to flow under its own gravitational force and can completely occupy the formwork, even when there is a high density of reinforcement present. According to the ACI-237R-07 [2], SCC is a type of concrete that is very fluid and does not separate. It can easily spread and fill the formwork, and it can cover the reinforcement without needing any mechanical consolidation. SCC, also known as self-placing concrete and self-levelling concrete, is a category that includes all subsets of SCC [2]. The proportion of aggregate in the total volume of the mixture is 70% [3]. Recycled aggregate (RA) can be utilized as either fine aggregate or coarse material. Recycled concrete, often known as RCA, refers to concrete that is formed from crushed old concrete. For recycled concrete aggregate the bulk density is lower than that of ordinary aggregate because it has a greater capacity to absorb water in its pores. Ultimately, it is necessary to develop an appropriate blend in order to ascertain the precise amounts needed for manufacturing concrete using RCA [4]. Torsional moment has experienced a surge in popularity in recent times, mostly due to the more space efficient, economical, and aesthetic requirements. Torsional moment impacts the structural integrity and flexibility of various architectural components, including spandrel beams, curved beams, elements subjected to off-center loads, spiral staircases, and box girders in bridges. Mohamad Ali [5] suggested new expressions to calculate the torsional strength and torsional stiffness for

spandrel beams under single and two concentrated loads and recommended to use of the ACI limit design method in designing the spandrel beams for torsion with no provision of longitudinal steel required to resist torsion. While Abdulridha [6] investigated thirteen specimens that were tested under pure torsion. Test results showed that, in the presence of steel plates, the behaviour of composite beams is different, and there is an enhancement to the resistance of the applied torque. Where the present study aims to experimentally and analytically investigate the torsional behaviour beams cast with self-compacting concrete which contains different percentage of recycled concrete aggregate. The parameters which will be considered include the RCA replacement ratios (0%, 25%, 50%, and 75%) of normal coarse aggregate, the type of cross-section beam, the amount of reinforcement, in addition to the results of the concrete mixture Fresh and Hard.

The study will investigate properties including the general behaviour of beams under pure torsion, cracking, ultimate torque, and the angle of twist. Qader [7] explored the response of concrete members to pure torsion. The experimental results compared nine reinforced Self-Compacting beams, divided into three groups. Each group contained beams, the first with a solid cross-section and the second with a hollow core. Two grades of steel reinforcing deformed bars were used in all beams. The use of hollow core beams resulted in reduced cracking and ultimate torque.

## 2. MATERIALS

The characteristics of the materials utilised in the

fabrication of the tested reinforced SCC beams with RCA are outlined as follows. The tests were conducted at the laboratories of the department of civil engineering at the University of Basrah.

## 2.1 Concrete

Four concrete mixes were utilised, varying based on the proportion of recycled concrete aggregate replacing natural material. Typically, chemical admixtures were used to achieve workable concrete with a low w/c ratio. Below is a concise

overview of the components utilised in the production of concrete.

### 2.1.1 Cement

Type I Ordinary Portland Cement (Mabroka) is a widely utilised cement type that is suited for all general concrete construction purposes. Hence, it was used in this work. This type adheres to the specified condition outlined in IQS 5-1984 [8]. Tables 1 and 2 provide properties of the chemical and physical, respectively.

**Table 1.** Cement physical characteristics

Physical Characteristics	Tests Results	Limits of Iraqi Specification No.5/1984
Fineness using Blaine air permeability apparatus (m <sup>2</sup> /kg)	316	≥ 230
Soundness (Autoclave), %	0.6	≤ 0.8
Setting time (Vicat's apparatus)		
Initial setting time, min.	125	≥ 45 min
Final setting time, min.	248	≤ 600 min
Compressive strength of mortar		
3 days, MPa	20.3	≥ 15
7 days, MPa	28.4	≥ 23

**Table 2.** Cement chemical profile

Oxide Composition	Content (%)	Limits of Iraqi Specification No.5/1984
CaO	62.25	-
SiO <sub>2</sub>	20.64	-
Al <sub>2</sub> O <sub>3</sub>	5.01	-
Fe <sub>2</sub> O <sub>3</sub>	3.58	-
MgO	2.4	≤ 5.0%
SO <sub>3</sub>	2.31	≤ 3.0%
L.O.I	1.86	≤ 4.0%
I.R	0.74	≤ 1.5%
c	0.88	0.66-1.02
Main Compounds (Bogue's equations)		
C <sub>3</sub> S	50.69	-
C <sub>2</sub> S	21.22	-
C <sub>3</sub> A	6.63	-
C <sub>4</sub> AF	10.57	-

**Table 3.** Characterization of fine aggregate

Sieve Size (mm)	Cumulative Passing %	Limitation of Iraqi Specifications No.45/1984, Zone2
10.0	100	100
4.75	97	90-100
2.36	86	75-100
1.18	72	55-90
0.60	51	35-59
0.30	16	8-30
0.15	3	0-10
0.075	2.2	0-3

### 2.1.2 Water

Unadulterated tap water was utilized in the mixing procedure for all concrete compositions, according to the prescribed proportions specified in the design. In addition, the concrete curing procedure involved using pure water, which was replaced every two days for a period of 28 days. The curing process involved immersing the control specimens, including cubes, cylinders, and prisms, as well as the beam specimens, in a water tank filled with fresh water. This was done to evaluate the mechanical properties of the concrete. The specimens were continuously submerged in water for the entire duration of the test.

### 2.1.3 Fine aggregate (sand)

The manufacturing of SCC mixes involved the utilisation of natural sand sourced from Zubair-Basrah, Iraq. The fine aggregate had a maximum size of 4.75 mm and had a smooth texture with a spherical particle form. The sand was rinsed twice and subsequently air-dried, for the purpose of removing unwanted materials. Table 3 displays the classification of sand. The results indicate that the sulphate content of the sand was within the limitations specified in Iraqi Specifications No. 45/1984 [8], where the value was equal to 0.33.

### 2.1.4 Coarse aggregate

Two types of coarse aggregate were used:

### (1) Gravel

Sanam Mountain location in the city of Basra offers natural crushed gravel (NCA) with a maximum size of 19 mm, the crushed coarse aggregate was washed, and then kept in an internal saturated and dry surface condition before being utilized. Where the results indicate that the coarse aggregate grading is within the requirements of Iraqi Specification No. 45/1984 [9], Table 4 shows the properties of the coarse aggregate used.

**Table 4.** Grading of coarse aggregate

Sieve (mm)	Percentage Passing by Weight (%)		Limitations
	RA	NA	
25.0	100	100	100
19.0	92	90	90-100
9.5	24	20	20-55
4.75	0	3	0-10
2.36	0	1	0-5
Sieve No. #200	0.2	0.5	As Max 0.5



**Figure 1.** RCA preparation

**Table 5.** Physical properties and chemical composition of coarse aggregate

Test Details	NA	RA	Limitations of IOS No.45/1984
Specific gravity	2.66	2.14	
Water absorption (%)	0.67	4.10	
Dry compacted density (g/cm <sup>3</sup> )	1.60		
Suphate content (SO <sub>3</sub> )	0.073%	0.048%	≤ 0.1%
Chloride content (Cl)	0.092%	0.037%	≤ 0.1%

### (2) Recycled concrete aggregate

RCA is prepared by crushing old concrete cubes under a compressive force of 25-32 MPa manually. The crushed concrete is divided into three parts with sizes 14 to 20, 10 to 14, and 5 to 10 mm using sieves as depicted in Figure 1. The

**Table 8.** Test results of steel reinforcement

Bar size Ø (mm) (Deformed)	Test results			ASTM A615/A615M- limits		
	Yield stress fy (MPa)	Ultimate Strength fu (MPa)	Elongation (%)	Yield Stress fy (MPa) Min.	Ultimate Strength fu (MPa) Min.	Elongation Min. (%)
8	468	622	11	420	620	9
10	490	623	12	420	620	9
12	505	648	13	420	620	9

### 2.3 Mixing procedure

Two types of self-compacting concrete were produced: one

grades and physical characteristics of RCA are shown in Tables 4 and 5, respectively.

#### 2.1.5 Superplasticizer (HRWR)

To produce SSC with and without recycled concrete aggregate a high-range water reducer must be used to satisfy the SCC requirement even with a low (w/c) ratio. The superplasticizer used in this work is a new generation modified polycarboxylate, which can be commercially named. GLENIUM51. This material is compatible with all types of Portland cement, free of chlorides, and compatible with ASTM C494 [10]. Ultra-ductile concrete shows better workability without separation. It also provides sufficient time for mixing, pouring, and finishing the final concrete surface.

#### 2.1.6 Limestone powder (LSP)

The self-compacted concrete was achieved by using a higher proportion of LSP in the mixture, which includes both cement and filler materials. This material is commonly referred to as AL-Gubra and is obtained from the local market. It is a white grinding material derived from limestone quarried from several places in Iraq, commonly employed in construction procedures. Tables 6 and 7 display the physical attributes and chemical makeup of LSP.

**Table 6.** Physical properties of limestone (LS)

Physical State	Powder. Crushed Stone
Colour	White to dark grey
pH	8-9 (aqueous solution)
Specific gravity	2,71 g/cm <sup>3</sup>
Decomposition temp	899°C

**Table 7.** Chemical composition of LSP

Oxide	Content %
CaCO <sub>3</sub>	87
Fe <sub>2</sub> O <sub>3</sub>	0.25
Al <sub>2</sub> O <sub>3</sub>	0.73
SiO <sub>2</sub>	1.38
MgO	0.12
SO <sub>3</sub>	0.80
L.O.I	6.49

### 2.2 Steel reinforcement

The current investigation utilised steel reinforcing bars with sizes of Ø8, Ø10, and Ø12 mm for both the longitudinal reinforcement and stirrups. Three samples of each bar diameter were subjected to testing utilising the available testing machine at the laboratory of the Civil Engineering Department at Basra University. where the properties of the reinforcing bars are presented in Table 8.

using natural coarse aggregates and the other using recycled concrete aggregates to partially replace the natural coarse aggregate.

Various replacement ratios (0%, 25%, 50%, and 75%) were employed to substitute the natural coarse aggregate with recycled aggregate. Table 9 shows the quantities of materials included in each type of mixture, and the highlighted mix (number two) was used in the present experimental program.

Where the concrete mixture was produced using a Rotary drum mixer with a capacity of 0.1 m<sup>3</sup>.

The process can be succinctly described as follows: First, a combination of cement, limestone powder, and aggregate was mixed together for a duration of 1 minute. Second, 80% of the mixing water was gradually contained in the mixture, and the mixing process was continued for an additional minute. Third, the remaining 20% of water mixed with the dissolved superplasticizer was slowly added to the mixture while

continuing to mix for an additional minute. To avoid the conglomerate in the mix and offer higher workability and a good consistency for the concrete mix, Fourth, the mixing process was extended for an additional duration of three minutes. Fifth, the mixture was allowed to sit undisturbed for a duration of three and a half minutes.

Finally, the mix was remixed for half a minute before being discharged to conduct fresh concrete testing and cast the specimens. For concrete mixes with recycled aggregate replacement, mixing took longer than expected. A quick mixing process must be considered to ensure a uniform distribution of the concrete components, especially the recycled aggregates.

**Table 9.** The trail mixes investigated

Trail Mix No.	Cement kg/m <sup>3</sup>	Filler LSP kg/m <sup>3</sup>	Water L/m <sup>3</sup>	F.A (Sand) kg/m <sup>3</sup>	Gravel kg/m <sup>3</sup>	GI.51 L/m <sup>3</sup>
1	408	175	180	805	813	4
2	385	166	171	769	896	4
3	351	151	181	755	944	3

Trail Mix No.	Average of Three Cubes Compressive Strength (MPa) 28 days age			
	0%	25%	50%	75%
1	41.1	40.5	38.6	36.1
2	41.9	40.9	37.3	35.4
3	34	32.9	32	29.9

### 3. BEAMS DETAILS

**Table 10.** Details of beam specimens

Beam Designation	RCA %	Longitudinal (mm)	Stirrups (mm)
H	0	-	-
HL	0	4Φ 12	-
HS	0	4Φ 12	Φ 8 @ 100
RH1	25	-	-
RH2	50	-	-
RH3	75	-	-
RHL1	25	4Φ 12	-
RHL2	50	4Φ 12	-
RHL3	75	4Φ 12	-
RHS1	25	4Φ 12	Φ 8 @ 100
RHS2	50	4Φ 12	Φ 8 @ 100
RHS3	75	4Φ 12	Φ 8 @ 100

The experimental program consists of twelve hollow concrete beams that were constructed and subjected to torsional moments for testing purposes. The beams feature a rectangular cross-section measuring 200 × 250 mm and are 1500 mm long with rectangular hollow cores of dimensions (60 × 110 mm). The factors taken into consideration include the content of RCA, which ranges from 0% to 75%. The specifications of the beams are depicted in Table 10, while the quantity of longitudinal reinforcement and the number of stirrups are presented in Figure 2.

### 4. LOADING FRAME

The loading frame consists of an I-section girder that transfers the load from the testing machine, developed to fit the designed models, to two I-section wing arms. These arms are bolted to the ends of the concrete beams as shown in Figures 3 and 4. The testing machine applies the load centrally to the middle of the main I-section steel arm, which then directly transfers the load to the wing arms, generating torque on the tested beam. The main steel arm is connected to the wing arms by hinges to allow free rotation. The load is precisely applied at the center of the main arm.

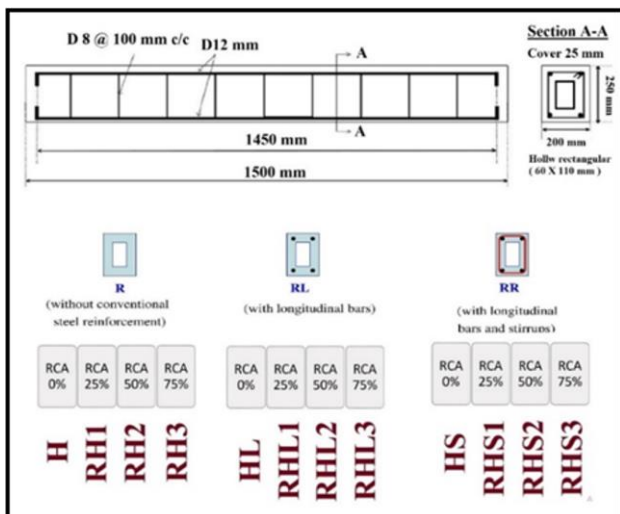


**Figure 2.** Typical hollow beam with overall dimensions



**Figure 3.** Test specimen

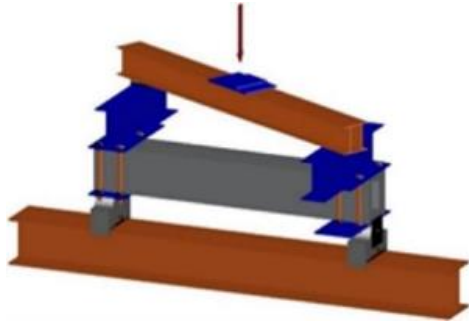


**Figure 4.** Steel frame and beam setup

## 5. CONCRETE PROPERTIES

### 5.1 Fresh state properties

The experimental program included selecting the appropriate concrete mixtures to obtain the best concrete properties required for self-compacted concrete; filling ability, passing ability, and segregation resistance. For these features to be guaranteed, several test methods were implemented. These properties of SCC in the fresh state were tested based on the procedure given by ACI237-R07.

#### 5.1.1 Slump flow and T50 slump test

Table 11 displays the outcomes of the slump flow test conducted on SSC samples with different amounts of RCA.

The results indicate that while the water-cement (w/c) ratio remains constant, the slump value of RAC reduces as the amount of RCA replacement increases during mixing. This implies that the stagnation flow decreases by varied percentages (3.54%, 7.8%, and 12.05%). The mixture comprises 25%, 50%, and 75% of coarse RCA.

**Table 11.** The results of Slump flow test

RCA%	Slump Flow (mm)	
	Measured	Limits
0	705	
25	680	650-800
50	650	
75	620	

The concrete's T50 slump flow time results for various amounts of RCA are provided in Table 12. As per the specifications and criteria provided by EFNARC [11]. The slump flow time of T50 was lowered by 25% while using 50% RCA. This is mostly caused by the decreased amount of typical coarse aggregate.

**Table 12.** The result of T 500 test

RCA%	T 500 (Second)	
	Measured	Limits
0	2.71	2 - 5
25	2.75	
50	2.96	
75	3.4	

#### 5.1.2 V-funnel flow time

Table 13 displays the outcomes of the funnel flow time V for the SCC mixture with varying RCA contents. The range of funnel flow time V is determined to be between 6.8 and 17.8

seconds. According to the EFNARC criteria and guidelines [12], the desired range for the funnel flow time V of SCC is between 8 and 12 seconds. Thus, the product of the funnel flow times V was inside the permitted range. High flow time can result from either limited flowability, which refers to the capability to fill or pass through, or flow obstruction [12]. The absence of cohesion can lead to the buildup of large particles in the conical discharge of a V-shaped funnel. This can result in the bending or curving of large particles, which can then obstruct the movement of concrete. The flow time dropped by 25% and 50% with the use of RCA, but experienced a considerable rise at 75% RCA.

**Table 13.** The result of V-funnel flow time

RCA%	V-Funnel (Second)	
	Measured	Limits
0	8.37	
25	8.55	8-12
50	9.13	
75	10.08	

#### 5.1.3 L-Box test

The L-Box test measures the passing ability of SCC. Also, segregation can easily be observed during the testing. The test results fall within the range of 0.8 to 1. The acquired result values conform to the approved norms of SCC. Table 14 displays the outcomes for Box L. It is worth mentioning that SCC mixtures lacking recycled concrete aggregate exhibit excellent flowability due to the smooth and spherical shape of the gravel particles. This shape allows the particles to slide effortlessly over one another.

**Table 14.** The result of L-Box test

RCA%	L-Box	
	Measured	Limits
0	0.95	
25	0.92	0.8-1
50	0.89	
75	0.76	

### 5.2 Hardened concrete test

#### 5.2.1 Density

Table 15 displays the mean densities of all mixtures after a period of 28 days.

**Table 15.** The result of density

RCA%	Density (gm/cm <sup>3</sup> ) at 28d
0	2.65
25	2.58
50	2.43
75	2.27

Analysis of the results generally indicates that the density of hardened concrete slightly decreased as the rate of natural coarse aggregate replacement by RCA increased, this was expected since the RCA presented a lower density compared to natural coarse aggregates due to higher porosity and lower density of cement past adhering to the aggregate surface.

#### 5.2.2 Compressive strength

Table 16 displays the average compressive strength results of three cubes at 28 days of age.

**Table 16.** Test result of compressive strength

RCA %	fcu MPa at 28 Day	$\frac{f_{cu}(RCA\%) - f_{cu}(0\%)}{f_{cu}(0\%)}$
0	42.1	0%
25	39.4	-6.4%
50	36.5	-13.3%
75	33.2	-21.1%

### 5.2.3 Splitting tensile strength

The occurrence of cracking in concrete is primarily attributed to tensile stress. The measured values of the splitting tensile strength test for all groups are presented in Table 17. The impact of different replacement ratios of natural coarse aggregate on Recycled Aggregate Concrete (RAC) is observed in terms of a loss in tensile separation strength. These ratios range from 6.7% to 23.4% after 28 days of curing for all combinations.

**Table 17.** Test result of splitting tensile strength

RCA %	ft MPa	$\frac{f_t(RCA\%) - f_t(0\%)}{f_t(0\%)}$
0	3.89	0%
25	3.63	-6.7%
50	3.29	-15.4%
75	2.98	-23.4%

### 5.2.4 Flexural strength

Table 18 indicates that the flexural strength of RAC (recycled aggregate concrete) decline as the proportion of natural coarse aggregate is replaced with recycled aggregate in the mixture. The percentage varied from 9.6% to 22.4% at the age of 28 days for all mixes. The presence of old mortar sticking to the aggregate particles in the recycled concrete aggregate can account for this phenomenon. The integration of new and ancient mortars is not seamless.

**Table 18.** Test result of flexural strength

RCA%	fr MPa	$\frac{f_r(RCA\%) - f_r(0\%)}{f_r(0\%)}$
0	4.37	0%
25	3.95	-9.6%
50	3.64	-16.7%
75	3.39	-22.4%

### 5.2.5 Modulus of elasticity (Ec)

**Table 19.** Test result of modulus of elasticity (Ec)

RCA %	Ec MPa	$\frac{E_c(RCA\%) - E_c(0\%)}{E_c(0\%)}$
0	27590	0%
25	25970	-5.9%
50	24540	-11%
75	23590	-14.5%

Table 19 displays the findings from testing conventional concrete and RAC. The results indicate that the modulus of elasticity in RAC is greater than in conventional concrete. Additionally, the modulus of ductility is influenced by the amount of RAC present, as it decreases with higher RAC content. It is also contingent upon the attributes and magnitude of the RAC content. The significant deformation of the RAC occurred due to a reduction in the elastic modulus of the RAC. The RAC replacement ratio of 25% and 50% results in a

reduction of the elastic modulus by 5.9-11% and a 75% replacement ratio leads to a reduction of 14.5% in the elastic modulus.

## 6. TEST RESULTS OF BEAMS UNDER TORSION

### 6.1 General behaviour of beams under loading and cracks patterns

Initially, cracks manifest on the vertical surfaces of the beam, and subsequently spread to all sides. Geometrically, the phenomenon can be referred to as torsion, while visible cracks manifest as crack torsion. Given that all the beams tested have rectangular sections, it follows that the initial formation of cracks can occur uniformly from one side.

With an increase in the load, further torsional cracks formed in the pure torsion span. When the maximum torque is applied, the number of diagonal cracks on each side grows and eventually forms a spiral shape until the specimen fails due to complete breaking caused by torsion.

Beams lacking longitudinal bars and stirrups exhibited cracking torque that was equivalent to the ultimate torque. These beams had no torsional ductility due to the absence of steel reinforcement in both the longitudinal and transverse directions, which would have provided resistance against the applied torque beyond the cracking stage. The beam experienced an abrupt failure, resulting in its separation into two distinct parts. This occurred when the initial cracks appeared, as depicted in Figure 5 (referred to as failure mode 'A').

**Figure 5.** Failure mode of beams (mode "A")



Figure 6. Failure mode of beams (mode “B”)



Figure 7. Failure mode of beams (mode “C”)

Figure 6 (failure mode "B") depicts beams that solely contain longitudinal bars. The beams exhibited brittle torsional failure, characterised by the development of a single intense helical crack. However, the presence of bars prevented the specimens from breaking into two separate pieces. Following the initial stage of cracking, one of the inclined individual cracks propagates and forms a spiral pattern around the surfaces of the member, gradually increasing in breadth until the point of collapse. By steadily increasing the load applied after the first cracking load, one of the inclined separate cracks expanded further along the beam until it reached the failure point known as the ultimate torque stage.

The beam's resistance increases after the initial breaking due to the presence of longitudinal reinforcing steel bars. This leads to an enhancement in the bonding of the concrete under loading, preventing a catastrophic collapse when the concrete reaches its ultimate tensile strength.

Structural elements reinforced with both longitudinal and transverse reinforcement. These exhibited a rise. The post-cracking behaviour leads to the creation of several helical and radial cracks.

In these instances, when the torque increased, the fissures expanded, grew in size, and became more noticeable. Ultimately, the beams broke, as depicted in Figure 7 (failure mode "C").

## 6.2 Cracking and ultimate loads

In this study, the prediction of pure torsion loading on beam specimens reveals two stages of behaviour, adopting a combination of two different theories. Initially, where no cracks form and the beams remain in the elastic state, the loading is described by a smeared crack analysis for plain concrete in torsion [13]. At the final stage, when loading reaches the maximum principal tensile stress of the concrete, the post-cracking behaviour is modeled by the well-known softened truss model [14-16], causing cracks to form and leading to the failure of an unreinforced member.

In the first stage, the load is resisted solely by the concrete. The addition of longitudinal steel without stirrups has little effect on the beam's strength under pure torsion, as it only helps resist the longitudinal component of diagonal tension forces. In the second stage, the load is resisted by a combination of both longitudinal and stirrup reinforcements. The cracking and ultimate load are detailed in Table 20.

Table 20. The results of the load of the tested beams

Beam Symbol	RCA% Content (i)	Cracking Load (Pcr)(kN)	Pcr i% / Pcr0% %	Ultimate Load (Pu) (kN)
H	0	3.975	3.975	100
HL	0	4.175	18.240	105
HS	0	4.400	18.966	111
RH1	25	3.492	3.492	100
RHL1	25	3.935	16.643	113
RHS1	25	3.929	17.612	112
RH2	50	3.421	3.421	100
RHL2	50	3.538	15.545	103
RHS2	50	3.646	17.994	106
RH3	75	2.692	2.692	100
RHL3	75	3.107	14.003	115
RHS3	75	3.150	16.107	106

Figures 8 and 9 show beam is tested by subsection to torsional moments. The loading of the specimens causes

certain changes in the behaviour as it transitions from the initial stage to the final stage. The cracking load is recorded as the load in which the cracks become visible to the recording camera by concrete crack width gauge.



Figure 8. Beam tested by subsection to torsional moments



Figure 9. The instruments used in the tests

### 6.3 Cracking and ultimate loads

Effect of RCA replacement ratio, by observing the results, no significant difference in behaviour was identified in the RCA-containing beams at the cracking stage, where all the beams exhibited similar linear torque-rotation behaviour. At the same time, RCA-containing beams show a decrease in cracking torque depending on the substitution ratio of RCA. The reduction in splitting tensile strength of RAC depends on what are the weak points between the binder and the old mortar in the RCA.

The torque is the moment that beams fail and cannot resist any increase in applied load. The ultimate capacity of the tested beam is determined by the highest torsional moment it can withstand. If the machine reading drops and the beam undergoes rapid deformation, it is considered a failure. Therefore, the cracking and ultimate torsional resistance of reinforced concrete members had been improved by adding steel although transverse reinforcement., such that any decrease in the machine reading accompanied by rapid deformation of the beam was described as failure.

Effect of longitudinal and transverse reinforcement, the load was applied on tested beam specimens up to failure. cracks manifested on the vertical surfaces and thereafter spread to all sides of the beam. Cracking torsion refers to the torsion level at which visible cracks become apparent. The augmentation in the initial fracture load for beams solely reinforced in the longitudinal direction, where the addition of longitudinal steel bars without stirrups has been effective in resisting the longitudinal component of the diagonal tension forces [17].

Where the results of the experimental test for beams showed that the effect of using transverse steel bars is clear with respect to the first cracking torsion resistance. the beams reinforced with transverse reinforcement demonstrated increment in both first cracking torque and ultimate torsional strength. This was due to the reinforcing steel being placed in an orderly manner in places exposed to tensile forces, which leads to an increase in the resistance of the material to bearing loads after it reaches the greatest tensile strength. cracking load but has a great effect on the ultimate load [16].

### 6.4 Torque - twist relationships

The angle of twist refers to the rotational displacement of the free end of a beam relative to its fixed end. Torsion occurs when a force is applied to a body, causing one end or part to rotate around a longitudinal axis while the other end or part rotates in the opposite direction. Table 21 illustrates the correlation between the torsion angle and the thresholds that were evaluated. Where the method used to calculate the angle of twist is performed by using a dial gauge attached to the bottom fiber of each end of the tested beam at a point (50 mm) from the centre of the longitudinal axis of the beam, as shown in Figure 9. The dial gauges recorded the downward displacement values to find the twist angle in radians, as follows:

$$\text{The angle of twist } (\theta) = \tan^{-1} \Delta/L \quad (1)$$

where,

$\Delta$ = dial gauge reading;

$L$ = distance from the centre of the beam to the position of the dial gauge = 50.

The test findings indicate that the relationship between torque and twist angle is linear until the occurrence of the first cracks. After that, the behaviour becomes nonlinear until the failure stage, which is referred to as TWIST. The twist angle was measured during the application of loads until the failure stage.

Table 21. Values of torque and corresponding angle of twist of beams

Beam Symbol	Cracking Stage		Ultimate Stage	
	Torque (kN.m)	Twist Angle (deg./m)	Torque (kN.m)	Twist Angle (deg./m)
H	1.292	0.044	1.292	0.044
HL	1.386	0.047	5.928	1.357
HS	1.430	0.052	6.164	2.328
RH1	1.135	0.041	1.135	0.041
RHL1	1.279	0.042	5.409	1.339
RHS1	1.277	0.045	5.724	2.189
RH2	1.112	0.038	1.112	0.038
RHL2	1.150	0.040	5.052	1.290
RHS2	1.182	0.043	5.648	1.946
RH3	0.915	0.031	0.915	0.030
RHL3	1.010	0.033	4.551	1.145
RHS3	1.024	0.036	5.235	1.912

The results of the angle of twist analysis indicate that the extent of concrete damage is directly influenced by the amount of replacement, with a corresponding increase observed as the replacement percentage rises. The beam experienced an increased impact due to an elevated twist immediately following cracking since the released energy resulted in a more

brittle crushing, as observed in Figures 10-12, whilst at comparison among beams that also have the same characteristics but with different reinforcement content, The result revealed that increasing the reinforcement content in the section will increase the value of the angle of twist of the beam clearly and result in an increase in stiffness, due to increasing the area under the curve (stiffness ) and the energy absorption capacity (ductility).is elucidated in Figures 13 and 14.

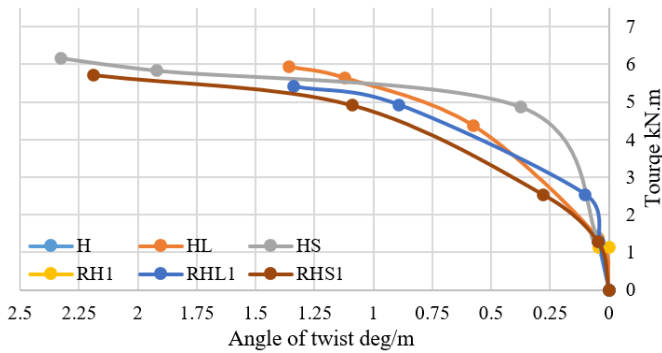


Figure 10. Torque-twist angle (RCA 25%)

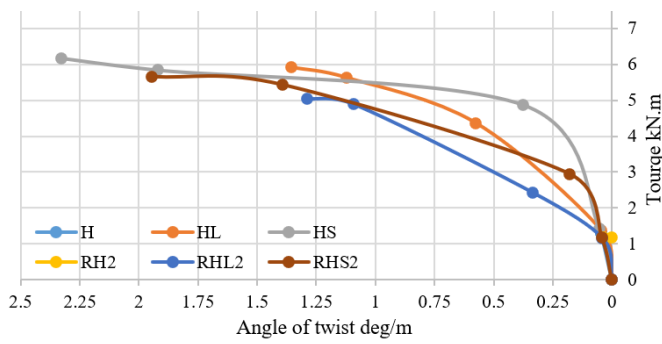


Figure 11. Torque-twist angle (RCA 50%)

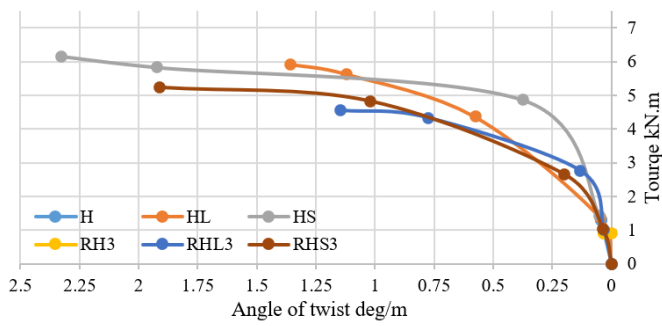


Figure 12. Torque-twist angle (RCA 75%)

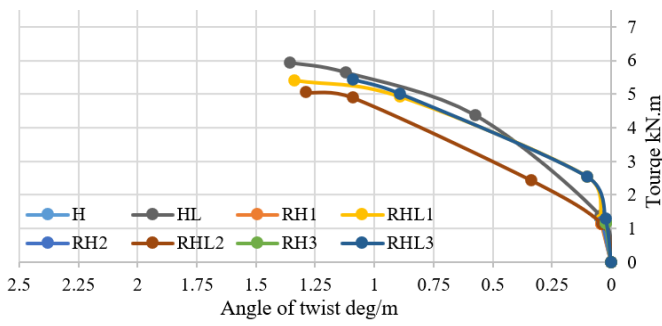


Figure 13. Torque-twist angle (beams with longitudinal reinforcement)

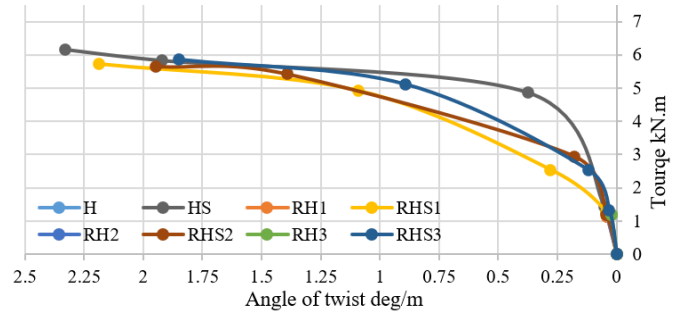


Figure 14. Torque-twist angle (beams with longitudinal and stirrups reinforcement)

The Figure 15 shows the results of cracking with the ultimate of the tested beams. At ultimate torque, the angle of twist increases due to the addition of reinforcement content, but still, the solid section has a smaller angle of about 13.89% when compared with hollow sections.

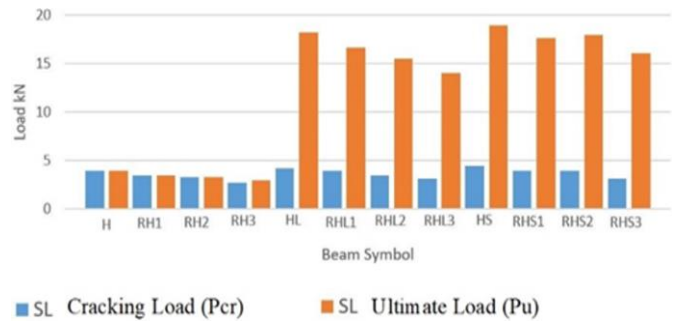


Figure 15. Loading (cracking, ultimate) for specimens

7. CONCLUSION

The test results allow for the formulation of the following conclusions:

1. The beam failed suddenly and separated into two parts as the first cracks developed, for plain beams without reinforcement. Where the cracking torque was equal to the ultimate torque.
2. The increase in the beam’s resistance after the initial cracking comes from the presence of longitudinal reinforcing steel bars, which led to an increase in the concrete’s bonding during loading and prevented the catastrophic collapse when the concrete reached the ultimate tensile strength.
3. The beams reinforced with transverse reinforcement demonstrated increment in both first cracking torque and ultimate torsional strength, the torque increased some of these cracks became excessively wide and beams failed by transverse steel yielding before concrete crushing.
4. No significant difference in behaviour was identified in the RCA-containing beams at the cracking stage, where all the beams exhibited similar linear torque-rotation behaviour. At the same time, RCA-containing beams show a decrease in cracking torque depending on the substitution ratio of RCA.
5. The angle of twist data suggest that the extent of concrete damage is directly influenced by the amount of replacement, with larger replacement percentages leading to increased damage.

6. Increasing the reinforcement content in the section will increase the value of the angle of twist of the beam clearly and result in an increase in stiffness.

## REFERENCES

- [1] Efnarc, S. (2002). Guidelines for Self-Compacting Concrete, European Federation for Specialist Construction Chemicals and Concrete Systems, Norfolk, UK. English ed.
- [2] ACI Committee 237 (2007). 'Self-consolidating concrete. Technical Documents, American Concrete Institute.
- [3] Rao, H.S., Reddy, V.S.K., Ghorpade, V.G. (2012). Influence of recycled coarse aggregate on punching behaviour of recycled coarse aggregate concrete slabs. *International Journal of Modern Engineering Research*, 2(4): 2815-2820.
- [4] Yang, K.H., Chung, H.S., Ashour, A. (2008). Influence of type and replacement level of recycled aggregates on concrete properties. *ACI Materials Journal*, 105(3): 289-296. <https://doi.org/10.14359/19826>
- [5] Mohamad Ali, A.A. (1983). Strength and behaviour of reinforced concrete spandrel beam. Doctoral thesis, University of Edinburgh.
- [6] Abdulridha, A.A. (2014). Structural Behaviour of strengthening reinforced concrete beams by steel plate under pure torsion. M. Sc. Thesis, Civil Engineering, College of Engineering, Al-Mustansiriya University.
- [7] Qader, S.S.A. (2019). Torsional behaviour of solid and hollow core self compacting concrete beams reinforced with steel fibers. *Engineering and Technology Journal*, 37(7): 248-255. <http://doi.org/10.30684/etj.37.7A.5>
- [8] Iraqi Standard No.5. (1984). Portland cement. The Central Organization for Standardization and Quality Control.
- [9] Iraqi Specification No. 45. (1984). Natural sources for aggregate that is used in concrete and construction. Baghdad.
- [10] ASTM. (2005). ASTM C494: Standard specification for chemical admixtures for concrete. West Conshohocken, PA, USA: ASTM.
- [11] Khayat, K.H. (1999). Workability, testing, and performance of self-consolidating concrete. *Materials Journal*, 96(3): 346-353.
- [12] ASTM C39/C39M-01 (2017). Standard test method for compressive strength of cylindrical concrete specimens. ASTM International.
- [13] Karayannis, C.G. (2000). Smear crack analysis for plain concrete in torsion. *Journal of Structural Engineering*, 126(6): 638-645. [https://doi.org/10.1061/\(ASCE\)0733-9445\(2000\)126:6\(638\)](https://doi.org/10.1061/(ASCE)0733-9445(2000)126:6(638))
- [14] Hsu, T.T., Mo, Y.L. (1985). Softening of concrete in torsional members-theory and tests. *Journal Proceedings*, 82(3): 290-303. <https://doi.org/10.14359/10335>
- [15] Hsu, T.T. (1996). Toward a unified nomenclature for reinforced-concrete theory. *Journal of Structural Engineering*, 122(3): 275-283. [https://doi.org/10.1061/\(ASCE\)0733-9445\(1996\)122:3\(275\)](https://doi.org/10.1061/(ASCE)0733-9445(1996)122:3(275))
- [16] Katkhuda, H.N., Shatarat, N.K., AL-Rakhameen, A.A. (2019). Improving the torsional capacity of reinforced concrete beams with spiral reinforcement. *International Journal of Structural and Civil Engineering Research*, 8(2): 113-118. <https://doi.org/10.18178/ijscer.8.2.113-118>
- [17] Ju, H., Lee, D.H., Kim, K.S. (2019). Minimum torsional reinforcement ratio for reinforced concrete members with steel fibers. *Composite Structures*, 207: 460-470. <https://doi.org/10.1016/j.compstruct.2018.09.068>